Fifth International Symposium on Marine Propulsors
smp'17, Espoo, Finland, June 2017

Development of New Type Low Drag Rudders in Propeller Slipstream

Takashi Kanemaru[1], Akira Yoshitake[1], Jun Ando[1]

[1]Faculty of Engineering, Kyushu University, Fukuoka, Japan

ABSTRACT

It is very important to estimate the interaction between propeller and rudder because the rudder in the propeller slipstream has the large effect on the propulsive performance. The propeller slipstream has the two characteristics produced by the working propeller. One is the velocity gradient in the axial direction by the accelerated flow and the other is the circumferential flow which does not contribute to the propulsive force. Many researchers have studied the propeller-rudder interaction problem and developed the unique rudders or energy saving devices added on the rudder in order to get the high propulsive performance including the rudder.

This paper presents the two kinds of newly developed rudders for the low drag and high performance. One is the swept back rudder to reduce the rudder drag produced by the velocity gradient and the other is the high thrust rudder with U-shaped notch which utilizes the circumferential flow to obtain the rudder thrust effectively. The rudder drag and the propulsive performance including these rudders are investigated numerically and experimentally.

Keywords

Propeller-rudder interaction, Low drag rudder, Rudder drag measurement, Propeller slipstream, SQCM

1 INTRODUCTION

The rudder behind the propeller has a great influence on not only the maneuverability but also the propulsive performance because of the propeller-rudder interaction. Since Yamagata & Kikuchi (1933) conducted the experimental research about the effect of rudder on the propulsive performance, many researchers studies the propeller-rudder interaction experimentally and theoretically (Nakatake et al 1978, Moriyama 1981, Moriyama and Yamazaki 1981, Tamashima et al 1992).

Recently the development and improvement of energy saving devices are conducted actively in order to reduce CO_2 emission. If we focus on the propulsive performance only, the rudder can be regarded as one of the energy saving devices that recover the energy from the circumferential flow produced by the working propeller, which does not contribute to the propulsion. Reaction rudder is well known and widely used as the low drag rudder which obtains the rudder thrust in the propeller slipstream.

This paper presents the two kinds of newly developed rudders which obtain the low drag effectively comparing with the conventional rudder. One is the swept back rudder (SBR) whose leading edge line is inclined backward linearly in the spanwise direction from its root section. The other is the high thrust rudder (HTR) which has U-shaped notch at the leading edge on the extended line of the propeller shaft center line.

In this study, the energy saving effects of these rudders are investigated numerically and experimentally. The calculation method for the propeller-rudder interaction applies our original surface panel method "SQCM" (Nakatake et al 1994, Ando et al 1995). Also the measurements of the propeller thrust, torque and rudder drag were conducted in the circulating water channel in Kyushu University. The calculated results comparing with the experimental data and the effect for energy saving by the present low drag rudders are shown.

2 RUDDERS

2.1 Rudder Drag in Propeller Slipstream

The rudder force in propeller slipstream consists of three components which are the drag by the viscosity, the drag by the pressure gradient and the rudder thrust. The latter two components are the characteristic forces due to the propeller-rudder interaction.

The propeller slipstream has the velocity gradient in the axial direction by the accelerated flow produced by the working propeller. Because of this, the pressure field behind the propeller has the negative gradient according to the positive gradient of the axial velocity in the propeller slipstream. As the result, the drag acts on the rudder in the propeller slipstream because the pressure field in the trailing edge side is lower than that in the leading edge side (**Figure 1**). This is the mechanism of the drag by the pressure gradient. If we focus on this component only, the rudder location as far from the propeller as possible is the best.

On the other hand, the rudder behind the propeller generates the thrust owing to the circumferential flow in the propeller slipstream. The inflow velocity vector at the rudder section has the attack angle as the composed

velocity vector from the axial and circumferential flow components and the forward component of the lift produced by the inflow with the attack angle becomes the thrust (**Figure 1**). The rudder thrust reduces the rudder drag and contributes to the propulsive performance.

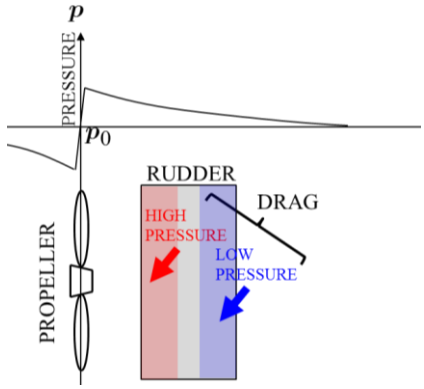

Drag by pressure gradiant

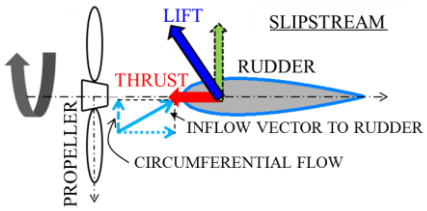

Rudder thrust

Figure 1 Rudder forces in propeller slipstream

2.2 Swept Back Rudder (SBR)

The arrangement of rudder which is far from the propeller is not realistic on the ship design though the rudder drag can be low. Instead of the backward arrangement, we propose the swept back rudder (SBR) which can keep the position of the rudder shaft and obtains the effect of the backward location at the rudder bottom side. SBR has the inclined leading edge line to backward linearly in the spanwise direction from its root section keeping the same chord length distribution of the conventional rudder. The rudder drag can be reduced without the design change of the ship stern. However the propeller thrust deduction caused by the decrease of the rudder displacement effect must be considered for the propulsive performance evaluation.

2.3 High Thrust Rudder (THR)

If we focus on the propeller performance only, the strong hub vortex is generally considered as undesirable phenomenon because of the large boss cap drag or the hub vortex cavitation. On the other hand, the hub vortex generates the rudder thrust because the circumferential flow around the hub vortex is very strong. However the hub vortex cannot keep flowing on the extended line of the propeller shaft center line because of the displacement effect of the rudder. So the contribution of the hub vortex to the rudder thrust is limited at the leading edge.

The high thrust rudder (HTR) has U-shaped notch at the leading edge on the hub vortex line in order to keep the circumferential flow component induced by the hub vortex as much as possible (**Figure 2**). Owing to the U-shaped notch, the hub vortex is not disturbed to the inside of the leading edge part and the rudder section around the hub vortex can get the large attack angle.

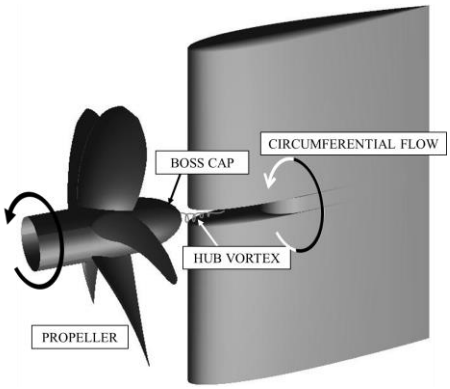

Figure 2 Outline of HTR

3 CALCULATION METHOD

The calculation method for the propeller-rudder interaction problem is based on a simple surface panel method "SQCM" (Nakatake et al 1994, Ando et al 1995). SQCM (Source and QCM) uses source distributions (Hess & Smith 1964) on the propeller blade surface and the rudder surface. Also discrete vortex distributions are arranged on their mean camber surfaces according to QCM (**Q**uasi-**C**ontinuous vortex lattice **M**ethod) (Lan 1974). These singularities should satisfy the boundary condition that the normal velocity is zero on the propeller blade surface, the rudder surface and their mean camber surfaces. In order to consider the effect of the hub vortex, hub vortex model (**Figure 3** (Kanemaru et al 2013)) for SQCM is incorporated in this calculation method. The calculation of the singularities on the propeller and the rudder is conducted simultaneously with the wake alignment which is important for the propeller-rudder interaction problem.

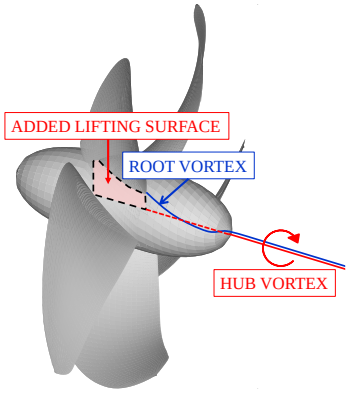

Figure 3 Outline of hub vortex model

The propeller coordinate system $o-xyz$ and the rudder coordinate system $o_r - x_r y_r z_r$ which is shifted from $o-xyz$ with the distance ℓ on the x -axis are introduced as **Figure 4**. The z_r -axis goes through the leading edge line of the rudder without swept back angle and attack angle.

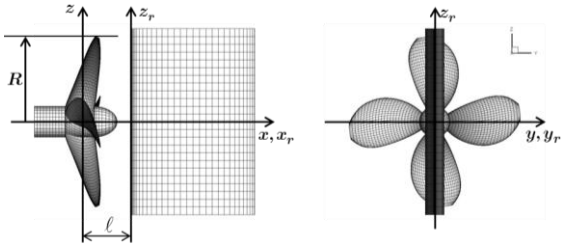

Figure 4 Coordinate systems of propeller and rudder

It is very difficult to calculate the singularity distribution on the rudder because of the singularity problem caused by the positional relation between the control point on the rudder and the vortex line on the wake sheet. We can overcome this problem introducing Rankine vortex model to Biot-Savart law which calculates the induced velocity by a vortex segment as shown by Equation (1) and **Figure 5**. The radius of the vortex core r_0 is assumed and the flow in r_0 is regarded as the rotation of solid body.

$$\vec{v}_\gamma = \frac{1}{4\pi}\frac{\vec{r}_1 \times \vec{r}_{12}}{|\vec{r}_1 \times \vec{r}_{12}|^2}\left\{\frac{\vec{r}_2}{|\vec{r}_2|} - \frac{\vec{r}_1}{|\vec{r}_1|}\right\}\cdot \vec{r}_{12} \qquad (1)$$

Where $\frac{|\vec{r}_1 \times \vec{r}_{12}|}{|\vec{r}_{12}|} = d$, if $d \le r_0$ then $d = r_0$

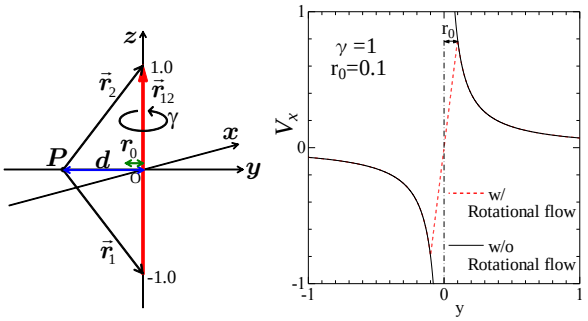

Figure 5 Induced velocity by a vortex segment

Rankine vortex model is very beneficial for the stable wake alignment and the elimination of the singular value on the rudder surface. Also Rankine vortex model is applied to the hub vortex with validated r_0 in order to obtain the rudder drag properly. In this method, r_0 is assumed as follows:

$$\begin{aligned} r_0 &= th(x_r) \quad (\text{ in rudder }) \\ r_0 &= 0.07R \quad (\text{ out of rudder }) \end{aligned} \qquad (2)$$

Where $th(x_r)$ and R are the thickness distribution of the rudder section and the radius of the propeller. In the realistic flow, the hub vortex might keep the small r_0 flowing the side of the rudder. However it is very difficult to express this phenomenon by the theoretical calculation method. We replace the phenomenon by considering that r_0 is enlarged by the rudder disturbance. Owing to this treatment, the rudder thrust limited at the trailing edge can be expressed.

The position vector $\vec{W}_{t\mu w}$ (**Figure 6**) at the time step number t can be decided by the movement from the previous position vector $\vec{W}_{t-1\mu w}$ as

$$\vec{W}_{t\mu w} = \vec{W}_{t\text{-}1\,\mu\,w\text{-}1} + \vec{V}_I \Delta t + \vec{V}_{St\mu w}\Delta t \qquad (3)$$

Where μ and ν are the position number in spanwise and chordwise direction, $\vec{V}_I$, Δt and $\vec{V}_{St\mu w}$ are the inflow velocity vector, time step and the induced velocity vector by the singularity distribution.

In this method, we use the unsteady model of SQCM (Maita et al 1997) in order to get the realistic wake sheet deformation including the rudder. The calculation method of unsteady propeller is described in the paper in detail.

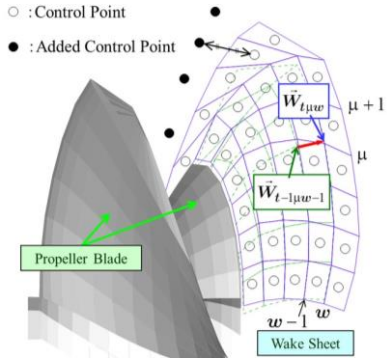

Figure 6 Movement of ring vortex nodes

The pressure on the rudder surface p_R can be calculated by the unsteady Bernoulli equation expressed as

$$p_R - p_0 = -\frac{1}{2}\rho(\vec{V}_r^2 - \vec{V}_{W_0}^2) - \rho\frac{\partial \phi_R}{\partial t} \qquad (4)$$

Where

p_0 : the static pressure in the undisturbed inflow

ρ : the density of the fluid

$\vec{V}_r$: the velocity vector on the rudder surface

$\vec{V}_{W_0}$: the velocity vector in the uniformed slipstream

ϕ_R : the perturbation potential on the rudder surface

The pressure coefficient C_{pn} is defined using the number of revolution n and the propeller diameter D as follow:

$$C_{pn} = \frac{p_R - p_0}{\rho n^2 D^2} \qquad (5)$$

The rudder drag F_x consists of the potential flow component F_{xp} and the viscous drag component F_{xv}.

$$F_x = F_{xp} + F_{xv} \qquad (6)$$

Where F_{xp} can be calculated by the pressure integration on the rudder surface as follow:

$$F_{xp} = \iint_{S_R}(p_R - p_0)\, n_x\, dS \qquad (7)$$

Where S_R and n_x are the rudder surface and the x component of the normal vector on S_R.

The calculation of F_{xv} uses the drag coefficient formula of NACA wing section presented by Abbott & Doenhoff (1949) as follow:

$$F_{xv} = \frac{1}{2}\rho\int_{z_s} C_{DR}(z)\,\bar{V}_{in\,x}^2(z)\,c(z)\,dz \qquad (8)$$

Where

$$C_{DR} = 0.012th/c + 2(1 + 2th/c)\,C_{f(Hughes)}$$

$$C_{f(Hughes)} = 0.066/(\log_{10} R_n - 2.03)^2$$

$$R_n = \frac{c(z)\bar{V}_{in\,x}}{\nu}$$

$\bar{V}_{in\,x}$ is the averaged inflow velocity to the x direction. $c(z)$ and th/c are the chord length and thickness ratio at the each rudder section.

The propeller thrust T_p and torque Q_p acting on the propeller blades are obtained by the pressure integration on the blades surface as follows:

$$T_p = \iint_{S_B} (p_B - p_0)\, n_x \, dS$$

$$Q_p = \iint_{S_B} (p_B - p_0)(n_y z - n_z y)\, dS \qquad (9)$$

Where S_B and p_B are the blade surface and the pressure on S_B. n_x, n_y and n_z are the x, y and z components of the normal vector on S_B.

Also the viscous components of the thrust and torque, T_v and Q_v are calculated by Nakamura's formula (1986) as follows:

$$T_v = -K\frac{1}{2}\rho\int_{r_H}^{r_0} C_{DB}(r)\overline{W}(r)\bar{V}_x(r)c(r)dr$$

$$Q_v = K\frac{1}{2}\rho\int_{r_H}^{r_0} C_{DB}(r)\overline{W}(r)\bar{V}_\theta(r)c(r)r\,dr \qquad (10)$$

Where

$$\overline{W}(r) = \sqrt{\bar{V}_x(r)^2 + \bar{V}_\theta(r)^2}$$

$\bar{V}_x(r)$ = x -component of velocity averaged in the chordwise direction

$\bar{V}_\theta(r)$ = θ -component of velocity averaged in the chordwise direction

r_H, r_0, $C_{DB}(r)$ and $c(r)$ are the radius of hub, the radius of propeller, the viscous drag coefficient and the chord length. $C_{DB}(r)$ is expressed as follow

$$C_{DB}(r) = C_{D_{\min}} \qquad (C_\ell < 0.2)$$

$$C_{DB}(r) = C_{D_{\min}} + 0.03(C_\ell - 0.2) \qquad (C_\ell \geq 0.2) \qquad (11)$$

Where

$C_{D_{\min}} = 0.0084 + 0.016t/c$, t/c : blade thickness ratio,

C_ℓ : sectional lift coefficient

The propeller advance ratio J, the propeller thrust coefficient K_T, the torque coefficient K_Q, the propeller efficiency η_P and the rudder drag coefficient K_{FX} are expressed as

$$J = \frac{V_A}{nD},\ K_T = \frac{T}{\rho n^2 D^4},\ K_Q = \frac{Q}{\rho n^2 D^5},$$

$$\eta_P = \frac{J}{2\pi}\frac{K_T}{K_Q},\ K_{FX} = \frac{F_x}{\rho n^2 D^4} \qquad (12)$$

Where V_A, T and Q are the advance velocity, the total thrust $T_p + T_v$ and the total torque $Q_p + Q_v$.

The calculated results in this paper are shown by the averaged value of one revolution. Furthermore we introduce the total efficiency η_{PR} considering that the rudder is a part of propulsion system as follow:

$$\eta_{PR} = \frac{J}{2\pi}\frac{(K_T - K_{FX})}{K_Q} \qquad (13)$$

4 EXPERIMENT

4.1 Models of Swept Back Rudder (SBR)

We select the rudder MR-2 in the study by Moriyama (1981) as the original rudder ('ORIGINAL' in **Table 1**) which has many informative data regarding the propeller-rudder interaction and made the models of ORIGINAL and two types of swept back rudder (SBR). One of the SBR has the inclined leading edge line with 10 degree to the vertical line, the other has the one with 20 degree (**Table 1**). **Figure 7** shows the photos of these rudders.

Table 1 Principal particulars of SBR

NAME OF RUDDER	ORIGINAL	SBR10	SBR20
CHORD LENGTH (m)	0.200		
SPAN LENGTH (m)	0.300		
ASPECT RATIO	1.50		
TYPE OF SECTION	NACA0015		
SWEPT BACK ANGLE (deg.)	0	10	20

ORIGINAL SBR10 SBR20

Figure 7 Model of SBR

4.2 Models of High Thrust Rudder (HTR)

We made the three types of high thrust rudder (HTR) model as shown in **Figure 8**. These are designed based on ORIGINAL (**Table 1**) and we focus on the effects of the depth and the width of the U-shaped notch. The maximum depth and width are 30% of the chord length and 10% of the span length considering both the rudder structure and the rudder performance for the maneuverability.

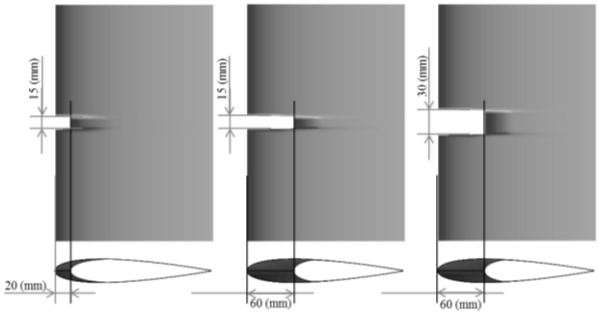

HTR10S HTR30S HTR30L

Figure 8 High thrust rudder (HTR)

4.3 Measurement of Rudder Drag behind Propeller

The measurements of the propeller thrust, torque and the rudder force in the propeller-rudder interaction were conducted in high speed circulating water channel of Kyushu University (**Figures 9**, **10** and **11**) in order to validate the propulsive performance with the present rudders and the calculation method. The drag of the rudder shaft can be eliminated by the shaft cover which have same wing section to the rudder. Also, the free surface cover makes it possible to measure the rudder drag without the wave resistance caused by the propeller open boat.

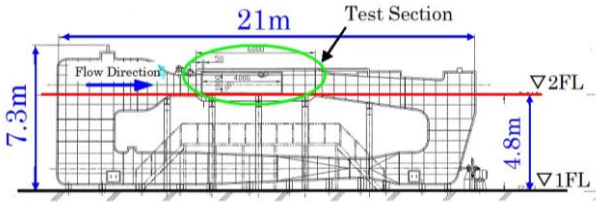

Figure 9 High speed circulating water channel

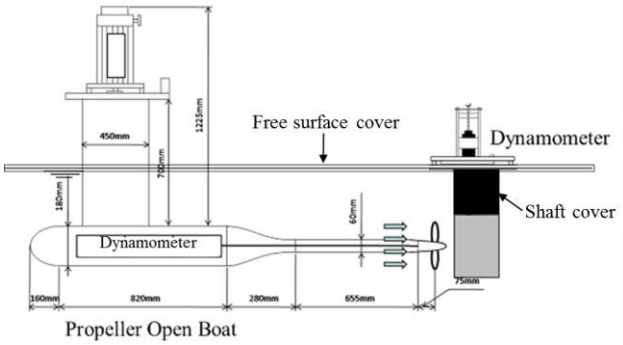

Figure 10 Measurement system

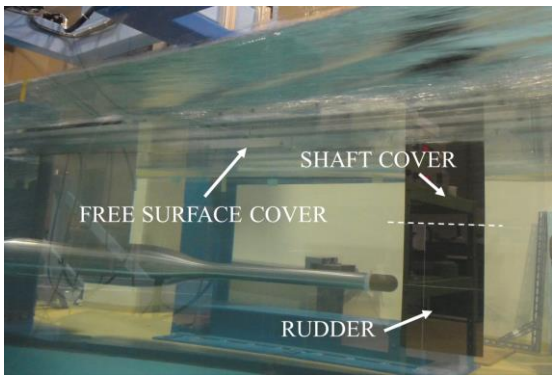

Figure 11 Test section in operating condition

We took the model propeller MP-B (**Table 2**) which was used in the propeller-rudder interaction study by Moriyama and Yamazaki (1981).

Table 2 Principal particulars of propeller

NAME OF PROPELLER	MP-B
DIAMETER (m)	0.2389
NUMBER OF BLADE	5
PITCH RATIO AT 0.7R	0.679
EXPANDED AREA RATIO	0.610
HUB RATIO	0.179
RAKE ANGLE (DEG.)	9.17
BLADE SECTION	AU

Figure 12 Model propeller MP-B

5 VALIDATION OF NEW TYPE LOW DRAG RUDDERS

5.1 Effect of Rudder for Propeller Performance

Figure 13 shows the experimental and calculated propeller performance with and without ORIGINAL. It is known that K_T and K_Q with rudder are larger than those without rudder by the displacement effect. The calculated results show the good agreement with the experimental data regarding this phenomenon. However, the calculated displacement effect is smaller than the experimental one. As the result, K_T and K_Q with rudder by the calculation are smaller than those by the experiment.

Figure 14 shows the change of K_T, K_Q and K_{FX} to the distance between propeller and rudder. The calculated result can express that the rudder drag becomes small by the backward location from the propeller.

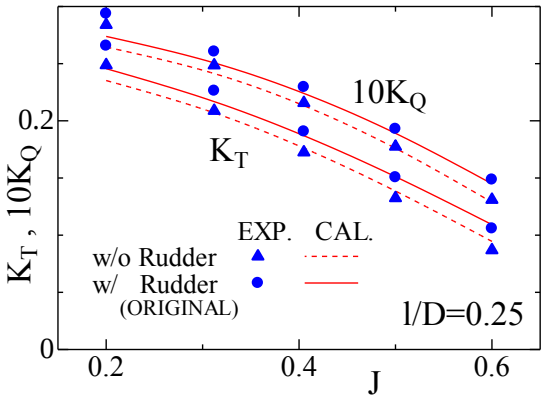

Figure 13 Propeller performance w/ and w/o rudder

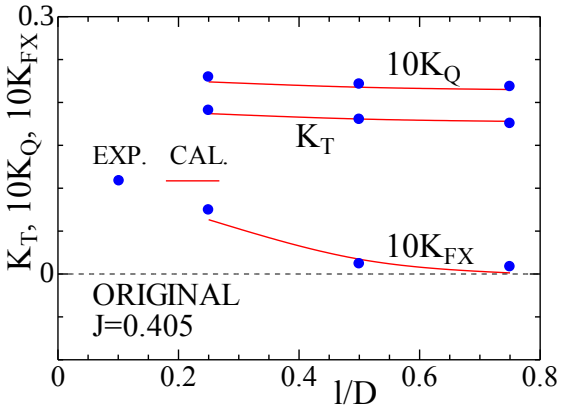

Figure 14 Rudder drag reduction by distance from propeller

5.2 Performance of Swept Back Rudder (SBR)

Figures 15 and 16 show the deformed wake sheet by the wake alignment in each advance ratio J and the calculated pressure distribution C_{pn} on the SBR. All calculated results in this paper get the converged wake sheet and the stable pressure without singularity.

Figure 17 shows the K_T, K_Q and K_{FX} in the propeller-rudder interaction regarding SBR. Both the calculated results and the experimental data show that SBR has the same effect to that the rudder is located far from the propeller. It can be seen that the thrust acts to the rudder in the case of high loading condition in the results of SBR20.

Figure 18 shows the total propulsive performance that the rudder is considered as a part of propulsion system. The difference of $K_T - K_{FX}$ is hardly seen because the K_T reduction and the K_{FX} reduction by the swept back of the leading edge are almost the same amount. On the other hand, the K_Q becomes small by the swept back. As the result, the total efficiency η_{PR} becomes larger in both the experimental data and the calculated results. We can see 1.2% up in the experiment and 1.5% up in the calculation regarding SBR20 comparing with ORIGINAL(**Figure 19**).

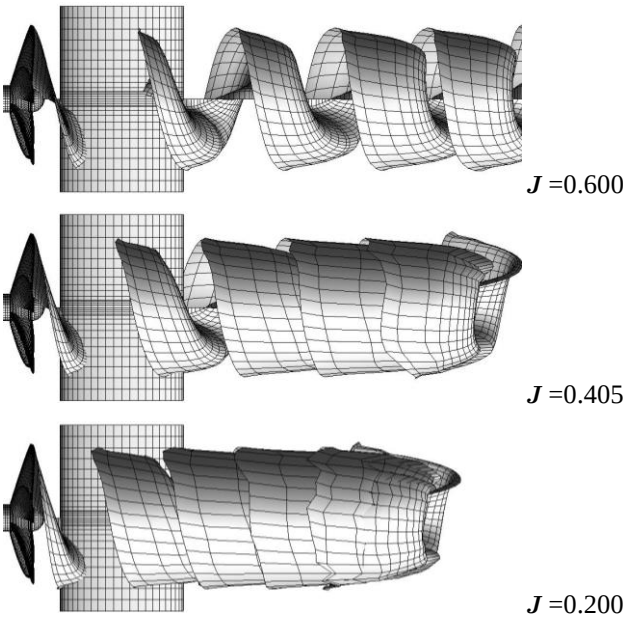

Figure 15 Deformed wake sheets with rudder (ORIGINAL)

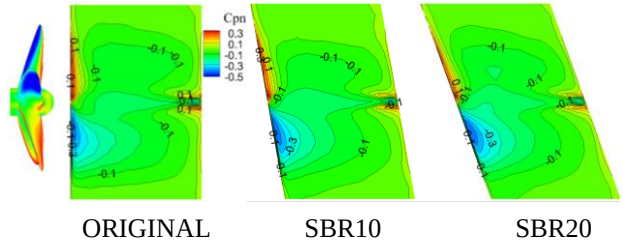

Figure 16 Pressure distribution on SBR (J =0.405)

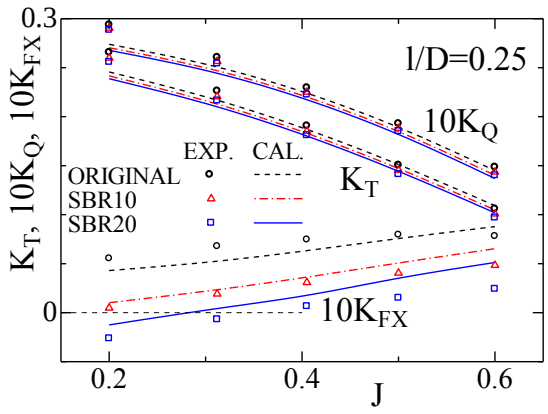

Figure 17 Results of propeller-rudder interaction of SBR

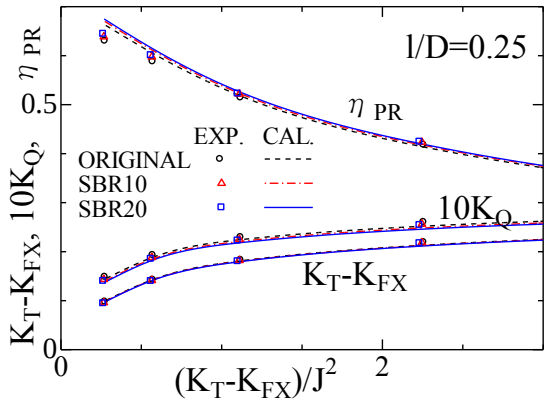

Figure 18 Propulsive performance of SBR

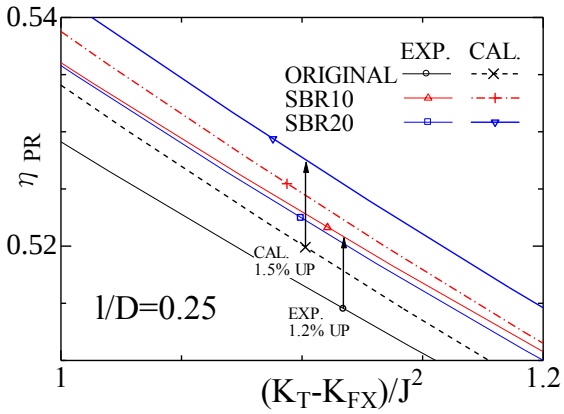

Figure 19 Effect of SBR for propulsive performance at design point

5.3 Performance of High Thrust Rudder (HTR)

Figure 20 shows the calculated pressure distribution C_{pn} on the HTR. It can be seen that the pressure at the section in U-shaped notch are different each other.

Figure 21 shows the rudder drag distribution in the spanwize direction $K'_{FX}(z)$.

$$K'_{FX}(z) = \frac{\Delta F_x}{2\rho n^2 D^3 \Delta z} \qquad (14)$$

Where ΔF_x is the rudder drag of the section with Δz which is the spanwise panel size at each section.

All results show the peak of the drag at the section on the extended line of the propeller shaft center line, namely, the hub vortex line because the section is in the hub vortex core which does not have the strong circumferential flow component. Except for these sections, the rudder thrust is produced around the hub vortex. One more important point should be focused in this figure. The rudder thrust at the knuckle section of the U-shaped notch in HTR is smaller than that of ORIGINAL because the section has the effect to be tip by the discontinuous chord length distribution. On the other hand, the local free vortex (**Figure 22**) makes the attack angle of the section in U-shaped notch larger comparing with the case of hub vortex only. This is the reason that the section in U-shaped notch obtains the larger thrust on the calculation.

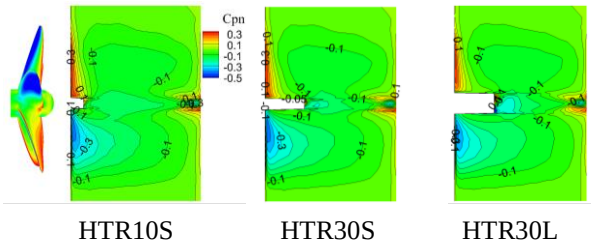

Figure 20 Pressure distribution on HTR (J =0.405)

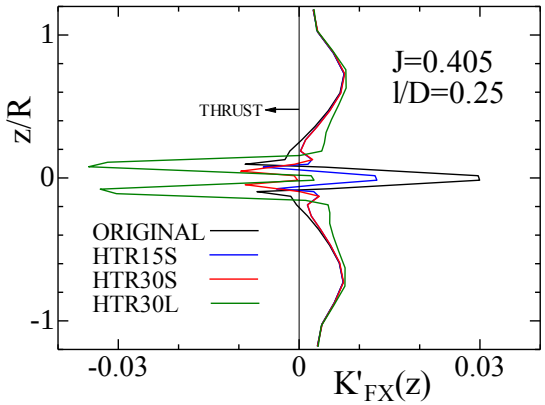

Figure 21 Rudder drag distribution of HTR

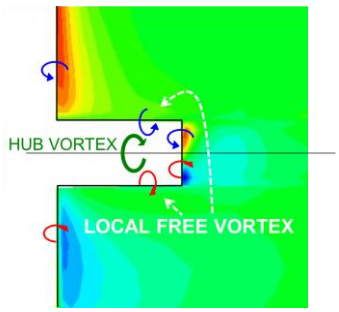

Figure 22 Local free vortex at U-shaped notch

Figure 23 shows the K_T, K_Q and K_{FX} in the propeller-rudder interaction regarding HTR. **Figure 24** extends the K_{FX} part in **Figure 23**. K_T and K_Q of all types of HTR are almost same to those of ORIGINAL. This result shows that the change of the displacement effect for the propeller by the U-shaped notch is very small. On the other hand, K_{FX} of HTR are smaller than that of ORIGINAL regarding both the experiment and the calculation. The calculated results show that HTR with deeper and wider notch obtains the lower rudder drag. However the differences of each K_{FX} in experimental data are small. We will investigate the reason in our future work.

Figure 25 shows the total propulsive performance that the rudder is considered as a part of propulsion system. The $K_T - K_{FX}$ and K_Q of HTR are larger and smaller comparing with ORIGINAL though the differences are small.

Figure 26 extends the total efficiency η_{PR} in **Figure 25**. 1.1% up in the experiment and 1.2% up in the calculation are obtained. However the types of HTR which obtain the lowest drag are different between the experiment and the calculation. HTR30L is the best in the calculated results but HTR30S is the best in the experimental data. We can see the contribution of HTR for the propulsive performance though some future works exist.

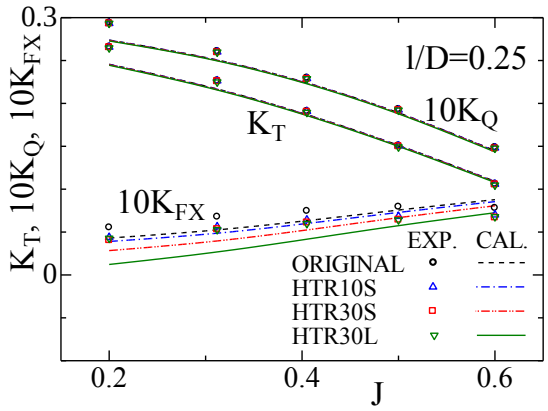

Figure 23 Results of propeller-rudder interaction of HTR

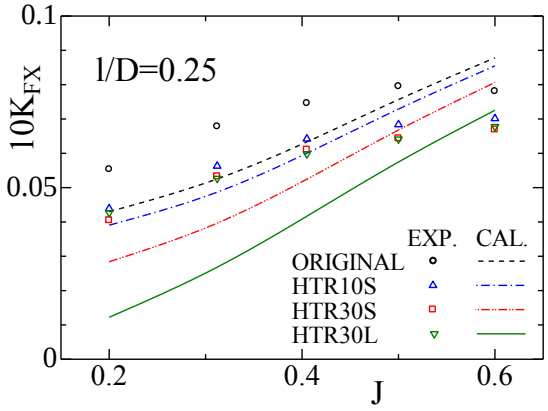

Figure 24 Rudder drag of HTR in slipstream

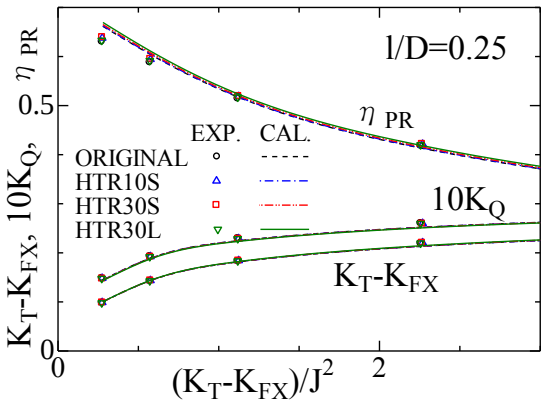

Figure 25 Propulsive performance with HTR

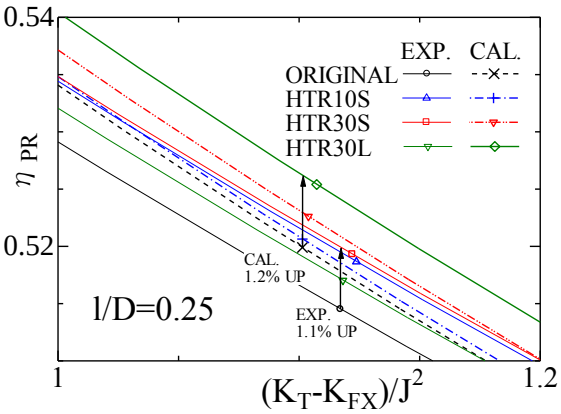

Figure 26 Effect of HTR for propulsive performance

6 CONCLUSIONS

In this paper, we present the two types of low drag rudders (SBR and HTR) which utilize the characteristic of the propeller slipstream and the propulsive performance with the propeller-rudder interaction are shown by the theoretical calculation and the experiment. SBR can obtain the effect of the backward location from the propeller and reduce the drag produced by the velocity gradient in the slipstream. Though the propeller thrust becomes smaller at the same time, the total propulsive efficiency including SBR is larger comparing with the original rudder. The displacement effect of HTR for the propeller is very small and HTR can obtain the high thrust owing to the U-shaped notch on the hub vortex line. As the results, the total propulsive efficiency is higher than that of the original rudder.

The performance of these rudders with attack angle such as the variation of the efficiency, the rudder normal force and the rudder torque will be studied in our future works. We are going to apply our calculation method to the practical rudder and modify these rudders for the better propulsion performance.

REFERENCES

Abbott, I. H., & von Doenhoff, A. E. (1949). 'Theory of Wing Section'. McGRAW-HILL.

Ando, J., Maita, S., & Nakatake, K. (1995). 'A Simple Surface Panel Method to Predict Steady Marine Propeller Performance'. Journal of the Society of Naval Architects of Japan **178**, pp.61-69.

Hess, J. L. & Smith, A.M.O. (1964). 'Calculation of Nonlifting Potential Flow about Arbitrary Three Dimensional Bodies'. Journal of Ship Research **8**(2), pp. 22-44.

Kanemaru, T., Ryu, T., Yoshitake, A., Ando, J., & Nakatake, K. (2013). 'The Modeling of Hub Vortex for Numerical Analysis of Marine Propeller Using a Simple Surface Panel Method "SQCM" '. Proceedings of 3rd International Synposium on Marine Propulsor, Launceston, pp.365-372.

Lan, C. E. (1974). 'A Quasi-Vortex-Lattice Method in Thin Wing Theory'. Journal of Aircraft **11**(9), pp.518-527.

Tamashima, M., Yang, D., & Yamazaki, R. (1992). 'A Study of the Forces acting on Rudder with Rudder Angle behind Propelle'. Transactions of the West-Japan Society of Naval Architects **84**, pp.37-48.

Nakamura, N. (1986). 'Estimation of Propeller Open-Water Characteristics Based on Quasi-Continuous Method'. Doctor thesis, Kyushu University.

Nakatake, K., Arimura, F., & Yamazaki, R. (1978). 'Effect of a Rudder on Propulsive Performance of a ship'. Transactions of the West-Japan Society of Naval Architects **55**, pp.13-25.

Nakatake, K., Ando, J., Kataoka, K. & Yoshitake, A. (1994). 'A Simple Calculation Method for Thick Wing'. Transactions of the West-Japan Society of Naval Architects **88**, pp.13-21.

Maita, S., Ando, J. & Nakatake, K. (1997). 'A Simple Surface Panel Method to Predict Unsteady Marine Propeller Performance'. Journal of the Society of Naval Architects of Japan **182**, pp.71-80.

Moriyama, F. & Yamazaki, R. (1981). 'On the Effect of Propeller on Rudder'. Transactions of the West-Japan Society of Naval Architects **61**, pp.25-39.

Moriyama, F. (1981). 'On the Effect of a Rudder on Propulsive Performance', Journal of the Society of Naval Architects of Japan **150**, pp.63-73.

Yamagata, M. & Kikuchi, Y. (1933).'Experiments on the Mutual Action between Propeller and Rudder'. Journal of the Society of Naval Architects of Japan **52**, pp.7-30.

DISCUSSION

Question from Luca Savio

The notch type rudder may postpone the formation of a cavitating hub vortex by extracting energy out of the vortex. Do authors think that this become other topic of hub vortex cavitation?

Author's closure

Thank you for your question. In this study, we focus on only the propulsive performance with rudder and the hub vortex cavitation is out of consideration. As our next step, we would like to study the effect by the high thrust rudder for hub vortex cavitation.